Oecologia (2015) 177:321–331
DOI 10.1007/s00442-014-3181-6

PHYSIOLOGICAL ECOLOGY - ORIGINAL RESEARCH

Growth maximization trumps maintenance of leaf conductance in the tallest angiosperm

George W. Koch · Stephen C. Sillett · Marie E. Antoine · Cameron B. Williams

Received: 17 June 2014 / Accepted: 2 December 2014 / Published online: 27 December 2014

Abstract Structural and physiological changes that occur as trees grow taller are associated with increased hydraulic constraints on leaf gas exchange, yet it is unclear if leaf-level constraints influence whole-tree growth as trees approach their maximum size. We examined variation in leaf physiology, leaf area to sapwood area ratio (*L*/*S*), and annual aboveground growth across a range of tree heights in *Eucalyptus regnans*. Leaf photosynthetic capacity did not differ among upper crown leaves of individuals 61.1–92.4 m tall. Maximum daily and integrated diurnal stomatal conductance (g_s) averaged 36 and 34 % higher, respectively, in upper crown leaves of ~60-m-tall, 80-year-old trees than in ~90-m-tall, 300-year-old trees, with larger differences observed on days with a high vapor pressure deficit (VPD). Greater stomatal regulation in taller trees resulted in similar minimum daily leaf water potentials (Ψ_L) in shorter and taller trees over a broad range of VPDs. The long-term stomatal limitation on photosynthesis, as inferred from leaf δ^{13}C composition, was also greater in taller trees. The δ^{13}C of wood indicated that the bulk of photosynthesis used to fuel wood production in the main trunk and branches occurred in the upper crown. *L*/*S* increased with tree height, especially after accounting for size-independent variation in crown structure across 27 trees up to 99.8 m tall. Despite greater stomatal limitation of leaf photosynthesis in taller trees, total *L* explained 95 % of the variation in annual aboveground biomass growth among 15 trees measured for annual biomass growth increment in 2006. Our results support a theoretical model proposing that, in the face of increasing hydraulic constraints with height, whole-tree growth is maximized by a resource trade-off that increases *L* to maximize light capture rather than by reducing *L*/*S* to sustain g_s.

Keywords *Eucalyptus regnans* · Growth maximization · Hydraulic balance · Leaf area to sapwood area ratio · Tree height

Introduction

From a hydraulic balance perspective, physiological and structural changes can compensate for the effects of gravity and increasing path length as trees grow taller, potentially sustaining a water supply to leaves that supports high stomatal conductance (g_s) and photosynthesis (Magnani et al. 2000; Whitehead and Beadle 2004; Ryan et al. 2006; Ishii et al. 2014). A reduced leaf area to sapwood area ratio (*L*/*S*), a lower minimum leaf water potential (Ψ_L), and increased wood specific conductivity are compensatory mechanisms observed in taller individuals of various tree species (Ryan et al. 2006). Within this hydraulic framework, reduced g_s in taller individuals is symptomatic of incomplete compensation and has been implicated in the slowing of height

Communicated by Nina Buchmann.

G. W. Koch (✉)
Center for Ecosystem Science and Society, Northern Arizona University, Flagstaff, AZ 86011, USA
e-mail: george.koch@nau.edu

S. C. Sillett
Department of Forestry and Wildland Resources, Humboldt State University, CA, Arcata 95521, USA

M. E. Antoine
Department of Biological Sciences, Humboldt State University, CA, Arcata 95521, USA

C. B. Williams
Department of Integrative Biology, University of California, Berkeley, CA 94720, USA

growth with tree height (*H*) and size (Ryan and Yoder 1997; McDowell et al. 2002b; Phillips et al. 2002; Delzon et al. 2004; Koch et al. 2004; Ambrose et al. 2010).

That increased *L*/*S* and other compensatory mechanisms are not consistently observed as trees grow taller (Ryan et al. 2006) has raised the question of whether maintenance of hydraulic balance and g_s is necessary to increase reproductive output and fitness as tree *H* increases (Becker et al. 2000; Thomas 2011). Using a growth model (DESPOT) that allocates carbon (C) to maximize C gain (Buckley and Roberts 2006a), Buckley and Roberts (2006b) determined that *L*/*S* should increase with *H*, despite a concomitant reduction in g_s. Increased allocation to *L* relative to *S* with *H* amounts to a shift in the balance of resource capture to light from water as the latter becomes more costly to acquire with increasing *H* and path length. Such a trade-off of resource acquisition can allow g_s to decline without reducing C gain, provided *L* increases sufficiently (Buckley and Roberts 2006b).

Although *L*/*S* declines with *H* in some species and conditions (McDowell et al. 2002a), there is a similar number of cases of increasing *L*/*S* with *H*, including for conifers (Whitehead et al. 1984; Long and Smith 1988; Callaway et al. 2000; Köstner et al. 2002) and angiosperms (Gerrish 1990; Vertessy et al. 1995; Phillips et al. 2002; Mokany et al. 2003). Within the optimal C gain framework of the DESPOT model, reduced *L*/*S* with *H* could arise from increased costs of nitrogen (N) or light with *H* growth, the former being indicated by declining leaf N with *H* and the latter resulting from light competition with neighboring crowns, reducing total light capture. Variation in the structures of real tree crowns, as influenced by competitive interactions and individual histories of disturbance, may affect relationships of *L*/*S* to *H* and growth. For example, trees with lower potential respiratory demands grew more than trees with higher potential respiratory demands per unit leaf area after accounting for the independent effects of tree size (Van Pelt and Sillett 2008; Sillett et al. 2010). Observations of reduced *L*/*S* with *H* may also indicate that optimal allocation (sensu DESPOT) is not possible, or that the model is incorrect.

In this study, we evaluate whether the growth maximization model of Buckley and Roberts or a hydraulic balance framework better fits observed changes in leaf physiology, *L*/*S*, and growth across a range of heights in *Eucalyptus regnans*. Giant eucalypts, including *E. regnans*, are among the fastest-growing trees, and they dominate forests with high C density (Keith et al. 2009). Their evolutionary history has been strongly influenced by fire (Tng et al. 2012), such that the avoidance of understory fires places a premium on height growth to raise seed capsules above the lethal zone.

As the tallest angiosperm, *E. regnans* is ideal for examining the influence of *H* on water relations, gas exchange, and hydraulic properties. Increasing *H* reduces leaf water potential and g_s in *E. regnans*, thereby explaining the lower stand-level transpiration in taller, mature forests compared to regrowth forests (Langford 1976). Leaf g_s is often lower in upper crown leaves of taller *E. regnans*, particularly on warmer days with higher VPD, suggesting that hydraulic constraints might limit growth in taller trees (Connor et al. 1977). Exceptionally high VPDs are associated with stomatal closure and steep Ψ gradients within trunks of *E. regnans* (Legge 1985). Thus, taller *E. regnans* experience and respond to greater hydraulic stress than shorter trees.

Compensatory changes in hydraulic properties with increased *H* also occur in tall *Eucalyptus*. Vessel diameter and wood specific conductivity near the tree base tend to increase with tree age and *H* (Mokany et al. 2003; England and Attiwill 2007), and xylem tapering in *E. regnans* exceeds the minimum theoretical tapering ratio required to prevent total path length resistance from increasing with *H* (West et al. 1999; Petit et al. 2010). In *E. delegatensis*, the increase in *L*/*S* with *H* is linked to greater wood specific conductivity (Mokany et al. 2003). Although there are no published data on *L*/*S* across a broad range of *H* in *E. regnans*, *L* and *L*/*S* increase with tree size (diameter) within a single age and height (~28 m) class, consistent with a growth rate benefit of higher *L*/*S* (Vertessy et al. 1995). Higher *L*/*S* is functionally related to higher growth rate in *E. nitens*, based on individual variation within a single height (<25 m) class (Medhurst and Beadle 2002).

Aboveground mass growth increases continuously with tree size in individuals nearing the maximum *H* known for *E. regnans* and *Sequoia sempervirens*, the tallest conifer (Sillett et al. 2010). Although upper crown foliage of taller individuals of *S. sempervirens* has lower g_s during both the wet and dry seasons (Ambrose et al. 2010) and operates with greater stomatal limitation of photosynthesis (Koch et al. 2004; Ambrose et al. 2009), this leaf-level constraint is not expressed as a slowing of biomass growth in taller individuals (Sillett et al. 2010). Here we ask if there is a similar relationship between *H* and leaf physiology in *E. regnans*, and how variation in leaf physiological constraints is related to variation in *L*/*S* with *H*. If maximization of whole-plant C gain (Buckley and Roberts 2006b), rather than maintenance of g_s, is the target of changes in allocation with increasing *H*, two patterns should be observed. First, taller trees should have higher *L*/*S* and lower g_s. Second, among individuals within a given height class, g_s should vary inversely with *L*/*S*, indicating that high leaf allocation relative to sapwood production necessarily leads to greater leaf-level hydraulic limitation. Both of these predictions should be realized if other factors (e.g., N availability) do not become increasingly limiting with *H* (Buckley and Roberts 2006b).

Methods

Site description

Our primary study site is located in the Wallaby Creek watershed, a 9,965-ha protected area on the southern edge of the Hume Plateau in King Lake National Park, Victoria, Australia (37°26′ S, 145°11′ E, ~690 m elevation). The forest is on the cool and dry margins of a Mediterranean climate. Long-term mean annual precipitation is 1207 ± 21 mm, and mean annual temperature is 11.6 °C, with below-average rainfall of 1,082 mm year^{-1} occurring during the period 1996–2006 (Australian Bureau of Meteorology 2007). Fog adds another 10–30 % to the annual precipitation total (Ashton 2000). Mean monthly maximum and minimum air temperatures are 28 and 6 °C in summer and 8 and 2 °C in winter, respectively (Australian Bureau of Meteorology 2007). Large day-to-day temperature fluctuations are common. Strong winds originating in the continent's hot, arid interior deliver desiccating conditions that poise the system for fire.

The forest canopy is dominated by *E. regnans*. With many trees over 85 m tall, and a few over 90 m, this was the world's tallest angiosperm-dominated forest (Van Pelt et al. 2004) prior to a stand-replacing fire in February 2009. Like many Australian ecosystems, the forest at Wallaby Creek is shaped by fire. Hanging streamers of peeled outer bark and highly combustible foliage make *E. regnans* forests prone to stand-replacing conflagrations. Not coincidentally, in the wake of such burns there follows a mass regeneration of *E. regnans* (Ashton and Chinner 1999), so this species commonly occurs in even-aged stands. The 80-year-old stand containing our "short" study trees dates back to 1926, when a large wild fire consumed the edges of the Wallaby Creek forest before being extinguished by a sudden shift in the weather (Ashton 2000). Stands containing trees in our 75-m and 90-m height classes regenerated after fires in 1851 and 1707, respectively. As of 2006, approximately 1,000 ha of old-growth *E. regnans* forest remained on the southeastern edge of the Hume Plateau, and our tallest study trees were located in a 299-year-old stand within this area. Prior to the tree-killing fire of 2009, these old *E. regnans* were extensively decayed, with numerous hollow trunks and limbs providing habitat for arboreal animals (Lindenmayer et al. 2000).

Tree measurements

In January 2005, we selected and measured five trees in each of three height and age classes (Table 1). The "tall" height class included trees within 5 % of the then tallest known *E. regnans*, with the "medium" and "short" trees being 4/5 and 2/3 the height of the tallest class. In this paper, we refer to the shortest, medium, and tallest height classes as 60, 75, and 90 m, respectively (Table 1). All study trees were dominants or co-dominants in their stands, were away from recently created gaps, and had unshaded upper crowns. Trees were rigged and climbed using standard rope techniques. In 2005, the entire aboveground portion of each study tree was exhaustively measured in three-dimensional space to quantify the area, mass, and volume of all major structural and functional components, including heartwood, sapwood, bark, cambium, and leaves (detailed methods in Sillett et al. 2010). Methods for quantifying leaf area and sapwood area are summarized here.

A sample of 16 foliar units and small branches was harvested to develop equations relating leaf area and leaf mass to branch diameter. A foliar unit was identified and defined as the aggregation of leaves on a branch system that was readily countable in the field. Increment cores were collected from the lower trunk, base of the live crown, and near the tree top on the main trunk. Multiple cores were taken at each height to account for variation in sapwood depth around trunk circumference. The heartwood/sapwood boundary was determined by applying a solution of methyl orange, which stains sapwood and heartwood differently. Sapwood area at the base of the live crown was used for calculating *L*/*S*. In 2006, we measured all trees again to enable the calculation of annual growth.

The majority of the field work described here occurred in 2006. Our study trees and nearly all *E. regnans* trees in the Wallaby Creek watershed died in the 2009 fire, which encompassed >400,000 ha. We returned to the site in March 2010 to search for and examine our study trees. At that time we climbed and collected trunk and branch wood samples along height gradients in four dead trees of the 90 m height class (see below).

Ongoing research on *E. regnans* provided comparable structural data for 12 additional trees, including seven from the Wallaby Creek forest sampled in 2002 (Van Pelt et al. 2004), three from Tasmania, one from Victoria, and one from New Zealand (S.C. Sillett and R. Van Pelt, unpublished data). These additional trees, which included the tallest and largest known *E. regnans* (Table 1), were nondestructively measured as described above and previously (Sillett et al. 2010).

Leaf photosynthetic capacity

Photosynthetic characteristics of upper crown leaves (~5 m from the treetop) of the 15 primary study trees were determined from light and CO_2 response curves using portable photosynthesis systems equipped with the 2 × 3 cm leaf chamber and red–blue LED light source (LI 6400, LiCor, Lincoln, NE, USA). Measured leaves were attached to foliar units that had been cut with a handsaw from the

Table 1 Vital statistics for 27 *Eucalyptus regnans* trees included in this study

Tree	Location	Year	Age (year)	Height (m)	fDBH (cm)	*L* (m^2)	*S* (cm^2)	PC1	PC2	Source
1[a]	Vic	2006	299	92.4	265	697	796	0.339	0.082	1
2[b]	Vic	2006	299	91.3	312	1,478	1,174	0.555	0.476	1
3[c]	Vic	2006	299	89.3	274	1,550	1,009	0.567	0.524	1
4[d]	Vic	2006	299	86.9	298	1,629	1,029	0.599	0.462	1
5[e]	Vic	2006	299	85.7	270	1,945	1,093	0.627	0.636	1
6	Vic	2006	155	78.1	241	705	620	0.225	0.659	1
7	Vic	2006	155	75.4	180	845	667	0.267	0.744	1
8	Vic	2006	155	75.4	145	668	606	0.192	0.710	1
9	Vic	2006	155	71.4	139	839	515	0.239	0.877	1
10	Vic	2006	155	70.9	162	424	528	0.120	0.473	1
11[a]	Vic	2006	80	64.7	115	842	515	0.212	0.993	1
12[c]	Vic	2006	80	64.1	97	412	515	0.077	0.762	1
13[d]	Vic	2006	80	63.8	80	295	465	0.000	0.777	1
14[b]	Vic	2006	80	62.2	113	515	647	0.122	0.831	1
15[e]	Vic	2006	80	61.1	95	532	496	0.104	0.962	1
16	Tas	2013	>300	99.8	383	2,898	1,787	0.817	0.729	2
17	Tas	2013	>200	91.2	264	2,419	1,151	0.627	0.929	2
18	Vic	2010	84	86.9	124	720	529	0.218	0.817	2
19	Vic	2002	295	85.1	241	766	748	0.327	0.320	1
20	Tas	2013	>400	84.2	551	3,313	2,761	1.000	0.499	2
21	NZ	2013	143	81.3	169	1,343	653	0.364	1.000	2
22	Vic	2002	295	80.8	218	770	870	0.321	0.339	1
23	Vic	2002	295	79.6	221	1,139	909	0.401	0.645	1
24	Vic	2002	295	79.2	245	735	731	0.331	0.254	1
25	Vic	2002	295	78.8	189	398	578	0.152	0.129	1
26	Vic	2002	295	75.6	176	528	778	0.228	0.172	1
27	Vic	2002	295	74.0	171	278	751	0.057	0.000	1

Estimated tree age, height, functional diameter at breast height (fDBH), leaf area (*L*), sapwood cross-sectional area at base of live crown (*S*), and first two principal components (PC1, PC2) from multivariate analysis of seven aboveground structural attributes (Sillett et al. 2010), listed along with data source. The first fifteen trees, which were sampled in 2006, and another seven trees (sampled in 2002) were from source 1 (Sillett et al. 2010). Five other trees from Victoria (Vic), Tasmania (Tas), and New Zealand (NZ) were from source 2 (S.C. Sillett and R. Van Pelt, unpublished data). *Superscripts* indicate trees paired during diurnal conductance measurements

upper crown, lowered to the ground, then recut underwater and allowed to equilibrate for at least 2 h, resulting in Ψ_L typically ≥ -0.4 MPa. This rehydration served to assess gas exchange capacity in the absence of height-related influences on Ψ_L, and thus g_s or photosynthesis. Leaf temperature was controlled at 26 ± 0.5 °C and VPD at 1.5 ± 0.2 kPa during CO_2 and light response curves. Leaves were exposed to a series of CO_2 concentrations with the chamber reference CO_2 set to the following series of ppm values: 400, 300, 200, 100, 75, 50, 400, 600, 90, 1,200, and 1,600. Each concentration was maintained until net CO_2 exchange stabilized (CV of assimilation rate $\leq$1 %). Light curves used a decreasing series of photosynthetic photon flux density (PPFD) values in the order 2,000, 1,600, 1,200, 900, 600, 300, 200, 100, 75, 50, 25, and 0 µmol m^{-2} s^{-1}, with readings taken manually when the net CO_2 exchange rate had stabilized. A minimum of two, and an average of three, leaves from the upper crown of each of the 15 study trees were measured for gas exchange characteristics. Gas exchange parameters were derived from A–C_i and *A*–light curves using an Excel tool developed by K. Tu (http://landflux.org/Tools.php) and based on Ethier and Livingston (2004).

Diurnal conductance and leaf water potential

Patterns of diurnal leaf conductance and water potential were compared in pairs of trees in the 60-m and 90-m height classes on seven sampling days in December 2006. All study trees were within 2 km of each other. Measurements on two days were abandoned because of rain and high winds; thus, 5 days of paired measurements are reported here. The day prior to measurements, we installed a working platform (Portaledge, Metolius, Inc., Bend, OR, USA) and a pressure chamber (model 1000, PMS Instruments, Corvallis, OR, USA) with a nitrogen tank within 5 m of the treetop of one 60-m and one 90-m tree. In each tree, five foliar units were selected and tagged for measurement. The next morning we returned to the trees, ascended in the dark, and sampled one leaf from each foliar unit to determine pre-dawn Ψ_L. Shortly after sunrise (~6:00), we began the first round of g_s measurements in each tree using a leaf porometer (Model SC-1, Decagon Devices, Pullman, WA, USA). Preliminary comparisons showed no difference in conductance between the two sides of pendant *E. regnans* leaves. The two porometers measured g_s similarly when compared via 34 paired measurements spanning a range of conductance values (17–241 mmol m^{-2} s^{-1}) on a variety of species growing in Kinglake National Park (paired *t* test, $p = 0.12$).

Prior to each conductance measurement, we measured PPFD both horizontally and in a plane parallel to the leaf using a quantum sensor (LI-189, LiCor Inc., Lincoln, NE, USA). Conductance values reported here are for measurements made on leaves with incident PPFD (normal to leaf surface) ≥400 µmol $m^{-2}s^{-1}$. About 1 h was required to measure g_s on three leaves from each of the five foliar units. Following each round of g_s measurements, Ψ_L was measured on one leaf from each foliar unit. This cycle of alternating g_s and Ψ_L measurements was repeated 7–8 times throughout the day until near sunset (~18:00). Temperature and relative humidity measurements recorded by the porometers were used to calculate vapor pressure deficit (VPD). Micrometeorological variables were also obtained from records logged by instruments on an eddy-covariance tower at the site (Kilinc et al. 2012). Maximum daily air temperature recorded by the porometers compared closely with those measured by the tower for the same days (porometer = tower ×0.972 + 0.298, $R^2 = 0.908$). Maximum VPD calculated via porometers averaged 0.8 kPa (±0.4 kPa) higher than that measured concurrently by the tower.

Physical and chemical analyses

In all 15 study trees, 8–10 upper crown leaves were collected for specific leaf area (SLA), leaf nitrogen (N), and carbon isotope composition (δ^{13}C). In the 90-m height class, 8–10 leaves were collected at 5-m height intervals within the crowns of each tree to examine height gradients of leaf properties. Wood was sampled from four trees in the 90-m height class. Using a chain saw, wedges (~20 cm deep by 20 cm wide by 8 cm thick) were cut from the main trunk and major branches at roughly 5-m height intervals. One upper crown branch was cut from each tree and lowered to the ground, where cross-sections were cut at 5-m height intervals and then progressively shorter intervals out to the tips of a tree top branch. Wedges were sanded and examined under a microscope to estimate the depth of the outermost 5 years of wood. Wood from this age range was sampled using a handsaw to cut a channel of uniform width, and the sawdust produced was collected. We followed a similar procedure for cross-sections of larger branches. For smaller branches with fewer than 5 years of growth, the entire cross-section was sampled. Leaf N and δ^{13}C were analyzed at the Colorado Plateau Stable Isotope Laboratory (http://www4.nau.edu/cpsil/). Samples were dried at 60 °C, ground to 40 mesh, and then a subsample was pulverized, encapsulated in tin, and combusted (CE Instruments NC 2100) at 1,000 °C. The resultant CO_2 was purified, and its $^{13}C/^{12}C$ ratio was analyzed by isotope-ratio mass spectrometry (Delta Plus XL, ThermoQuest Finnigan) in continuous-flow mode. The δ^{13}C values were expressed as the relative abundance of ^{13}C vs ^{12}C compared with a standard (Pee Dee Belemnite): $\delta^{13}C = (R_{sam}/R_{std} - 1) \times 1000$ ‰, where R_{sam} and R_{std} are the $^{13}C/^{12}C$ ratios in sample and standard, respectively. The standard deviation of repeated measurements of secondary standard material was <0.1 ‰ (external precision).

Statistical analyses

Variation in leaf physical, chemical, and gas exchange characteristics and whole-tree *L*/*S* across tree height classes was analyzed by ANOVA with means compared by Tukey–Kramer HSD test via JMP (version 11.0, SAS Institute, Cary, NC, USA). Height gradients of leaf SLA, N, and δ^{13}C within crowns of 90-m trees were examined by linear regression. Diurnal time series of g_s and Ψ_L were fitted with second-order polynomial equations, which were then integrated over the daytime period (~6:00–18:00) and used to calculate the integrated g_s and Ψ_L. Diurnal maxima of g_s and minima of Ψ_L for 60-m and 90-m trees were compared via paired *t* tests. A value of $P < 0.05$ was used to define statistical significance.

We used an information-theoretic approach to test the hypothesis that *L*/*S* increases with *H* as predicted by Buckley and Roberts (2006b). We began by defining a model to predict *L*/*S* using *H* and orthogonal dimensions of crown structure identified by principal components analysis of seven aboveground structural variables (i.e., leaf area, cambium area, green bark volume, total dry mass, cambium-area-to-leaf-area ratio, green bark volume to green bark area ratio, and sapwood volume to leaf area ratio) in 27 trees. As described by Sillett et al. (2010), the first two principal components of this analysis were highly significant, with PC1 expressing a tree's overall size and PC2 expressing the balance between a tree's respiratory demands and its photosynthetic capacity. Principal components scores were relativized so that values ranged from 0 to 1 prior to modeling. After defining a saturated model including all three predictors (i.e., *H*, PC1, PC2), we compared simpler models on the basis of likelihood, AIC_c, and Akaike weights (Wagenmakers and Farrell 2004). Statistical model fitting proceeded in R (R Foundation for Statistical Computing, Vienna, Austria).

Table 2 Mean (standard deviations) values of structural, chemical, and physiological properties of upper crown leaves (8–10) from *Eucalyptus regnans* trees of three height classes

Height class (m)	SLA (m^2 kg^{-1})	N (mg g^{-1})	$\delta^{13}C$ (‰)	A_{max} (μmol m^{-2} s^{-1})	R_d (μmol m^{-2} s^{-1})	g_{max} (mol m^{-2} s^{-1})
90	4.60^a	18.0^a	−26.11^a	15.3^a	1.9^a	0.19^a
	(0.78)	(1.8)	(0.58)	(2.1)	(0.3)	(0.04)
75	5.25^a	16.7^a	−27.57^b	16.0^a	2.0^a	0.23^a
	(0.66)	(1.7)	(0.38)	(1.8)	(0.2)	(0.03)
60	5.19^a	17.4^a	−27.38^b	17.2^a	1.5^a	0.22^a
	(0.44)	(2.1)	(0.60)	(1.4)	(0.7)	(0.02)

SLA specific leaf area, *N* leaf nitrogen concentration, $\delta^{13}C$ carbon isotope composition, A_{max} light-saturated photosynthesis, R_d leaf dark respiration, g_{max} stomatal conductance at light saturation

Within columns, *means followed by different letters* differ significantly ($P < 0.05$)

Results

Upper crown leaves from the different height classes were similar for all gas exchange parameters and leaf features except for δ^{13}C, which was higher in 90-m trees compared to 75-m and 60-m trees (Table 2). Within the crowns of 90-m trees, leaf δ^{13}C increased with H (Fig. 1), there being a 5–10 ‰ increase from the lowest to highest leaves (Appendix A). Treetop leaf δ^{13}C of 75-m and 60-m trees was within the range of values observed at equivalent heights in the crowns of 90-m trees (Fig. 1). For a given H, wood δ^{13}C was higher than leaf δ^{13}C and showed no trend from the tree base to about 70 m, above which it increased with H (Fig. 1). Leaf N (mg g^{-1}) increased significantly with H within the crowns of three trees in the 90-m height class ($N = 0.046 \pm 0.010 \times H + 14.5 \pm 1.4$, $P < 0.03$; Appendix B). Treetop leaf N in the 75-m and 60-m trees was within the range of values observed at equivalent heights in the crowns of 90-m trees (data not shown).

Predawn Ψ_L was slightly lower in 90-m than in 60-m trees, but minimum Ψ_L did not differ between height classes on any measurement day (Fig. 2). Minimum Ψ_L varied among days, ranging from −1.7 MPa on December 12 to −2.4 MPa on December 9. In 60-m and 90-m trees, minimum Ψ_L was linearly and similarly related to maximum daily VPD (Fig. 3).

Daytime g_s was generally higher in 60-m than in 90-m trees (Fig. 2), with the daily maximum g_s averaging 36 % higher in the shorter height class across the 5 days (174 ± 21 mmol m^{-2} s^{-1} vs 129 ± 22 mmol m^{-2} s^{-1}, $P = 0.045$). Integrated over the day (Fig. 4), g_s averaged 34 % higher in 60-m than in 90-m trees ($P = 0.002$). In both height classes, integrated g_s was a strong function of the daily maximum VPD (Fig. 4). In the shorter height class, g_s increased with maximum VPD, but in the taller trees, the relationship was nonlinear, with the highest g_s occurring on days with intermediate values of maximum VPD (Fig. 4, upper curves). Integrated only over the afternoon period (12:00–18:00), g_s declined similarly with maximum daily VPD for both height classes.

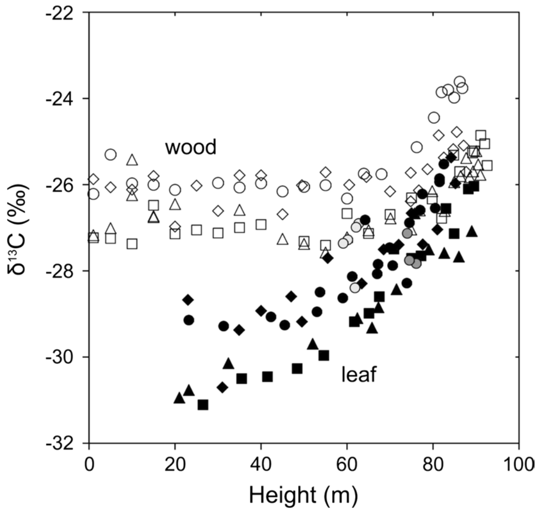

Fig. 1 Height gradients of leaf and wood δ^{13}C for *E. regnans* trees in 90-m (*black and white*), 75-m (*dark gray*), and 60-m (*light gray*) height classes. *Unfilled* (wood) and *filled* (leaf) *symbols* of a given shape are for the same trees

L/*S* increased with *H*, especially after accounting for size-independent variation in crown structure (Fig. 5). Regardless of *H*, trees with lower respiratory demands per unit photosynthetic capacity (i.e., higher PC2 scores) had higher *L*/*S* than trees with lower PC2 scores. The best model, which included parameters for *H* and PC2, was 36 times more likely than the best model excluding *H* (Table 3). The saturated model included a parameter for PC1 (tree size) in addition to PC2 and *H* and was less likely than the best model, even though it explained slightly (1.7 %) more variation in *L*/*S* (Table 3). Evidence for an additional effect of PC1 was not strong enough to provide a precise coefficient estimate (Table 3), which was not surprising considering the collinearity of PC1 and *H* ($R^2 = 0.57$).

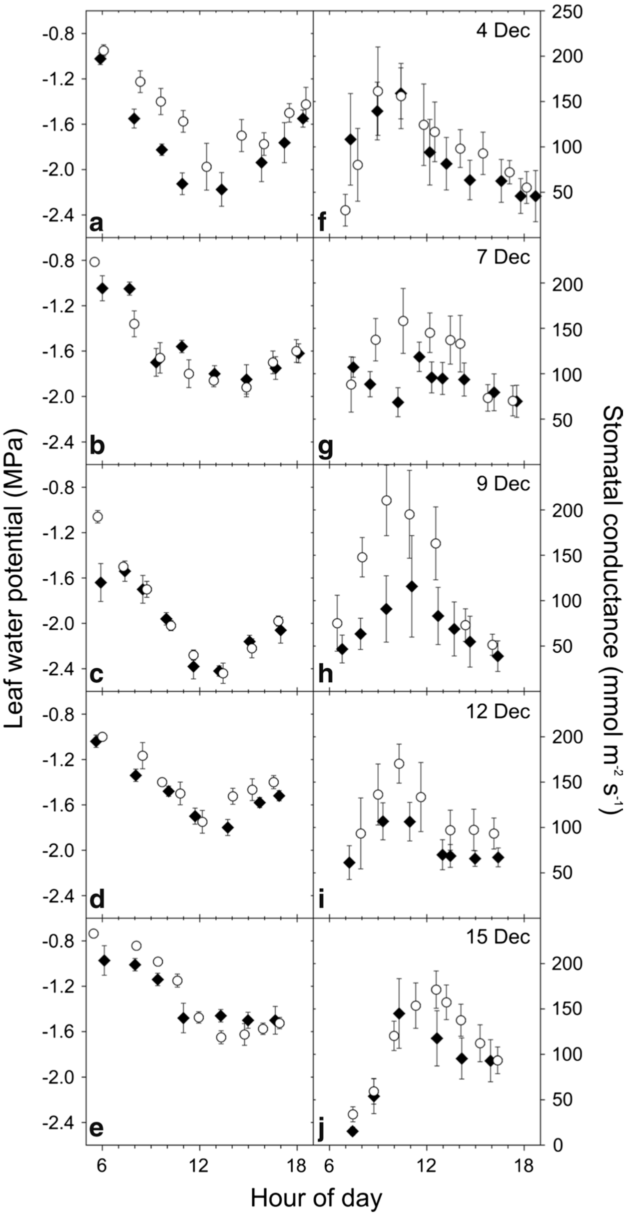

Fig. 2 Diurnal leaf water potential (Ψ_L; panels **a–e**) and conductance (g_s; panels **f–j**) in the upper crown of 60-m (*white circles*) and 90-m (*black squares*) tall *E. regnans* for 5 days in December 2006. Different trees of each height class were sampled on different days. Means ± 1SD

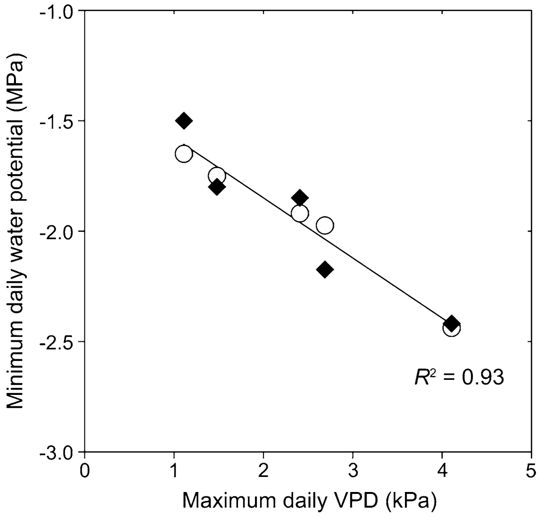

Fig. 3 Minimum leaf water potential in 60-m (*white circles*) and 90-m (*black squares*) tall *E. regnans* trees vs maximum daily VPD

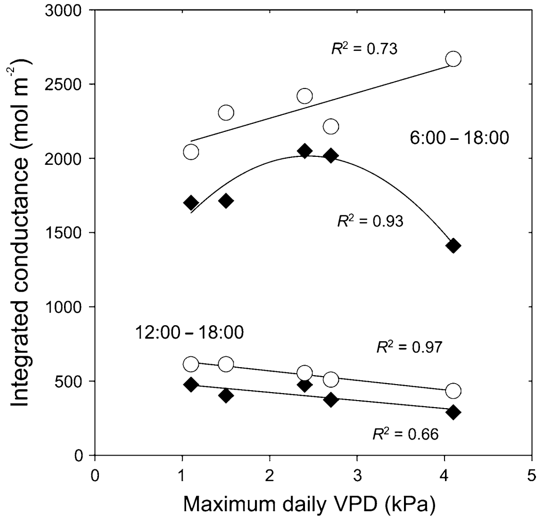

Fig. 4 Integrated diurnal conductance for 60-m (*white circles*) and 90-m (*black squares*) tall *E. regnans* trees vs daily maximum VPD. *Upper two curves* are for conductance integrated from 06:00 to 18:00 h, and *lower two curves* are for conductance integrated from 12:00 to 18:00 h

Discussion

With increasing tree height in tall *E. regnans*, whole-tree hydraulic architecture and leaf physiology varied in a manner consistent with the growth maximization model of Buckley and Roberts (2006b): *L*/*S* increased and g_s decreased with *H*, the latter based both on direct measurements and inferred from leaf δ^{13}C (Table 2). The physiological capacity of upper crown foliage did not differ across height classes, as indicated by the similarity of leaf N and gas exchange characteristics for leaves relieved of water stress. That leaf N did not vary indicates that N limitation did not increase with tree height in *E. regnans* at this site, and did not constrain the light-for-water resource acquisition trade-off proposed by Buckley and Roberts (2006b).

Lower g_s of upper crown leaves in taller *E. regnans* is consistent with many species (Ryan et al. 2006), including the tallest gymnosperm, *S. sempervirens* (Ambrose et al. 2010). Given the similar physiological capacity of upper crown leaves across tree heights, a lower g_s indicates that

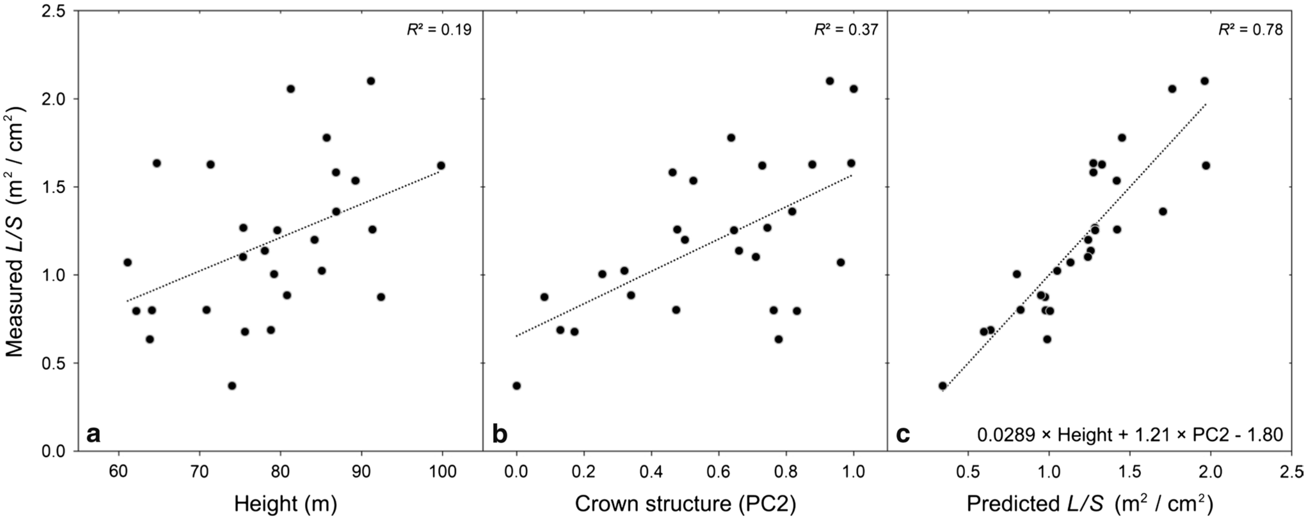

Fig. 5 Leaf area to sapwood area ratio (*L*/*S*) predicted by tree height (**a**) and crown structure (**b**) in *E. regnans* up to 99.8-m tall. Crown structure defined by second principal component (PC2) from multivariate analysis of seven aboveground structural attributes for 27 trees. PC2 tree scores scaled from 0 (highest demand/supply ratio) to 1 (highest supply/demand ratio), where demand is expressed as tissue quantities of inner bark, cambium, and sapwood, and supply is expressed as surface areas of leaves and photosynthetic bark (Sillett et al. 2010). Best model predicting *L*/*S* is shown on the right (**c**) along with the corresponding equation (see Table 3)

Table 3 Summary of models for predicting *L*/*S* of 27 *Eucalyptus regnans* trees (see Table 1) using tree height (*H*) and the first two principal components (PC1, PC2) from multivariate analysis of seven aboveground structural attributes (Sillett et al. 2010)

All possible models					Best model				
Model	*K*	AIC$_c$	w_i	R^2	Parameter	PC1	PC2	*H*	Intercept
+PC2 +*H*	4	0.458	0.598	0.779	Estimate	–	1.21	0.0289	−1.80
+PC1 +PC2 +*H*	5	1.336	0.386	0.796	SE	–	0.15	0.0043	0.38
+PC1 +PC2	4	7.648	0.016	0.711	% Variance	–	36.7	41.2	–
+PC2	3	26.053	0.000	0.367	Second-best model				
+PC1	3	27.022	0.000	0.344	Parameter	PC1	PC2	H	Intercept
+PC1 +*H*	4	29.796	0.000	0.344	Estimate	0.384	1.13	0.0214	−1.29
+*H*	3	32.581	0.000	0.194	SE	0.278	0.159	0.0069	0.524
Null	2	35.863	0.000	0.000	% Variance	1.7	36.7	41.2	–

Left side shows models ranked by Akaike weights (w_i). Predictors are sequenced by importance and noted for positive (+) or negative (−) correlations with *L*/*S*. Number of estimated parameters (*K*), selection criterion (AIC$_c$), Akaike weights, and goodness of fit (R^2) are given for each model. Right side shows parameter estimates, standard errors (SE), and % variance explained for the two best models

hydraulic constraints increased with *H* and path length in *E. regnans*. This was most evident when evaporative demand was highest, such as on December 9 (Fig. 2). When maximum VPD was ~4 kPa, there was a large difference between 90-m and 60-m trees in maximum and integrated g_s (Fig. 4). On days with lower VPD, g_s differed less between height classes, but was still consistently lower in the 90-m trees. The higher δ^{13}C of the upper crown foliage of 90-m trees compared to 60-m trees (Table 2) indicates greater stomatal limitation of photosynthesis in the taller trees over extended periods, and reinforces the interpretation of height-related differences in g_s based on porometry. Highly variable weather conditions on the Hume Plateau benefited this study by delivering a wide range of temperature and VPD conditions over a period when soil moisture in the rooting zone of *E. regnans* varied little, as indicated by similar predawn Ψ_L across measurement days.

The close similarity of the relationship between minimum daily Ψ_L and maximum VPD (Fig. 3) in 90-m and 60-m trees is consistent with strong regulation of g_s to maintain Ψ_L at or above a common set point. We observed no indication that taller *E. regnans* have a lower minimum Ψ_L, as has been observed in taller individuals of some species (Ryan et al. 2006). Consistent with this, our measurements of xylem vulnerability characteristics found no difference between branches from the upper crowns of 90-m and 60-m trees in the Ψ initiating loss of hydraulic conductivity or causing a 50 % loss of conductivity (C. Bentrup, unpublished data).

Patterns of wood δ^{13}C along the height gradient in 90-m trees (Fig. 1) provide insights into the distribution of whole-crown carbon assimilation in giant trees. Individual variation in wood δ^{13}C paralleled that of leaf δ^{13}C; trees with lower wood δ^{13}C at a given height also had lower leaf δ^{13}C. The lack of within-tree variation in wood δ^{13}C below 70 m was striking and contrasted with the strong height gradient in leaf δ^{13}C throughout the crown. This suggests that most of the photosynthate used for trunk wood growth originated near the tree top, where leaf δ^{13}C was similar to wood below 70 m. Based on our earlier detailed analysis of crown structure (Sillett et al. 2010), over 20 % of the total leaf mass is located within 10 m of the tree top in the 90-m trees. Given its higher light exposure, it is reasonable to conclude that this region of the crown, which included the zone used for diurnal g_s and Ψ_L measurements and comparisons of leaf physiological capacity, provided a disproportionate share of the photosynthate exported to the main stem and root system.

The growth maximization model of Buckley and Roberts (2006b) predicts that *L* and *L*/*S* should increase with *H* and that this should be at the expense of the maintenance of g_s. We found strong support for this prediction in the positive relationship between *L*/*S* and *H* and between *L*/*S* and leaf δ^{13}C. The *L*/*S* vs *H* relationship was significant ($P < 0.02$), but *H* alone explained only 19 % of the variation in *L*/*S* (Fig. 5a). Individual *E. regnans* trees of similar heights possess wide crown-level structural variation that is independent of tree size and closely related to the aboveground proportions of energy-demanding tissues (i.e., cambium, inner bark, and sapwood) compared to those supplying energy via photosynthesis (i.e., leaves and green bark). This energy balance metric—defined as the second principal component (PC2) from multivariate analysis of seven aboveground structural attributes (Sillett et al. 2010)—correlated significantly with *L*/*S* such that more vigorous trees (i.e., those with lower respiratory demands per unit photosynthetic capacity) had higher *L*/*S* than less vigorous trees (Fig. 5b). Including both *H* and PC2 greatly improved the model (Fig. 5c), with those variables explaining 41 and 37 %, respectively, of tree-level variation in *L*/*S* (Table 3). We conclude that it may be unrealistic to expect a strong relationship between *L*/*S* and *H* or any single size-related metrics among trees growing in natural stands, where crown structures are shaped by individual histories of disturbance and competitive interactions.

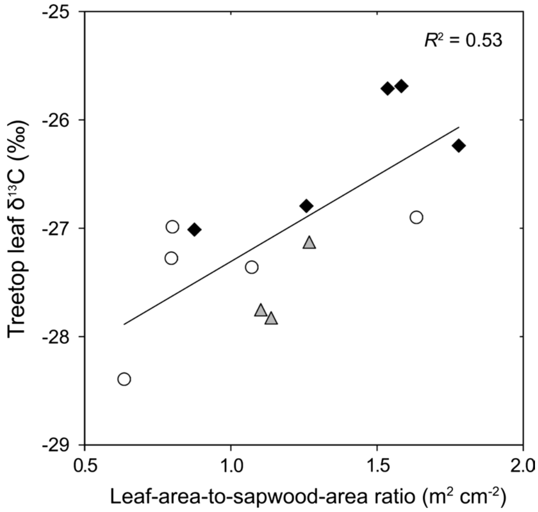

Fig. 6 Tree top leaf δ^{13}C vs leaf area to sapwood area ratio for *E. regnans* trees in 60-m (*white circles*), 75-m (*gray triangles*), and 90-m (*black squares*) height classes

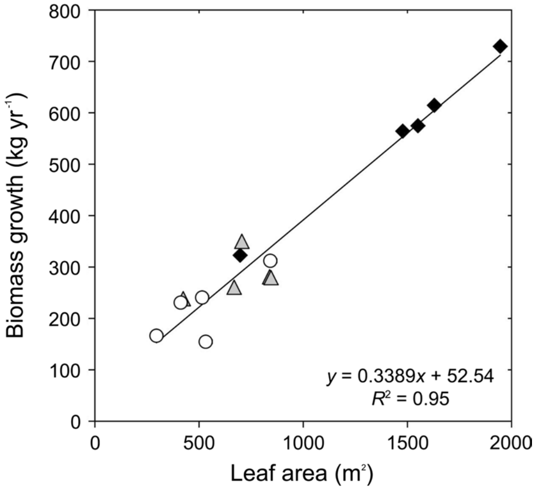

Fig. 7 Aboveground annual biomass growth vs total tree leaf area for *E. regnans* trees in 60-m (*white circles*), 75-m (*gray triangles*), and 90-m (*black diamonds*) height classes

The functional trade-off between *L*/*S* and leaf gas exchange performance is supported by the positive relationship of leaf δ^{13}C to *L*/*S* (Fig. 6), a pattern expected if increased allocation to *L* comes at the expense of maintaining hydraulic supply to upper crown foliage. Including *H* as a predictor in a multiple regression did not improve the model in Fig. 6, emphasizing the importance of *L*/*S* apart from *H* in regulating integrated water relations of upper crown leaves. In *E. regnans*, vessel diameter and wood specific conductivity near the tree base both increase with *H* (England and Attiwill 2007), and xylem tapering exceeds the minimum theoretical tapering ratio required to prevent total path length resistance from increasing with *H* (Petit et al. 2010, C. Williams, unpublished data). These apparent compensatory changes do not avert height-related declines in g_s. Rather than considering the lower g_s in taller *E. regnans* as symptomatic of incomplete hydraulic compensation, we interpret it as consistent with an ecological strategy that maximizes leaf area production to enhance C gain, growth rate, and reproductive output. This view is reinforced by analysis of structural and growth measurements (Sillett et al. 2010), which shows that 95 % of the variation in annual biomass growth increment is explained by total leaf area (Fig. 6).

Our previous study demonstrated that wood production increases with tree age and size in *E. regnans* and *Sequoia sempervirens* (Sillett et al. 2010) (Fig. 7). The present study helps explain how this occurs in *E. regnans*. Leaf area and *L*/*S* both increase with tree size, and although this may incur leaf-level reductions in photosynthesis during periods of atmospheric (or soil) moisture stress, it also confers enormous growth capacity. Given the high fire-risk environment of *E. regnans* and other *Eucalyptus* species, the capacity for rapid height and size growth may be of greater evolutionary advantage than the ability to avoid leaf-level impacts of episodic water stress.

The relationship of hydraulic architecture to branch- and leaf-level physiology has dominated studies of tree height and size growth. Understanding the adaptive significance of these patterns requires a whole-tree perspective (Ryan et al. 2006) and well-defined hypotheses regarding the evolutionary constraints of size-related development (Buckley and Roberts 2006b). The present study indicates that maximization of growth rate, rather than maintenance of g_s, is the target in *E. regnans*, a relatively short-lived species of giant tree. Regardless of age, large trees have tremendous growth potential and remain responsive to environmental changes (Latham and Tappeiner 2002; McDowell et al. 2003; Phillips et al. 2008; Sillett et al. 2015). The adaptive significance of this plasticity may well determine the fate of such trees as anthropogenic changes drive increased tree mortality worldwide (van Mantgem et al. 2009; Lindenmayer et al. 2012; Das et al. 2013).

Acknowledgments This research was supported by grants from the National Science Foundation (IOS-0445277 and IOS-1010769) and the endowment creating the Kenneth L. Fisher Chair in Redwood Forest Ecology at Humboldt State University. Comments by Mike Ryan and two anonymous reviewers improved the manuscript. We thank Tom Greenwood, Giacomo Renzullo, Jim Campbell-Spickler, Joe Harris, and Robert Van Pelt for help with tree climbing and sampling, and Jason Beringer and Darren Hocking of Monash University for providing micrometeorological data from the Wallaby Creek eddy-covariance tower. Russell D. Kramer helped with statistical analysis using R. We are especially grateful to Ion Maher and Tony Fitzgerald of Kinglake National Park, Victoria, for research permission, hospitality, and logistical assistance.

Appendix A

Linear regression equations of leaf δ^{13}C versus height for 90 m trees

Tree	Slope, ‰ m^{-1}	Intercept, ‰	*N*	R^2	*P*-value
1	0.0834	−33.907	15	0.937	0.00001
2	0.0529	−32.147	13	0.939	0.00001
3	0.0710	−32.249	15	0.867	0.00001
4	0.0494	−30.822	9	0.714	0.0001
5	0.1052	−34.426	12	0.888	0.00001

Appendix B

Linear regression equations of leaf nitrogen versus height for 90 m trees

Tree	Slope, mg g^{-1} m^{-1}	Intercept, ‰	*N*	R^2	*P*-value
1	0.0560	14.320	15	0.470	0.005
2	0.0150	15.254	14	0.127	0.23
3	0.0359	15.995	15	0.409	0.01
4	0.0241	16.137	11	0.160	0.20
5	0.0450	13.135	12	0.421	0.03

References

Ambrose AA, Sillett SC, Dawson TE (2009) Effects of tree height on branch hydraulics, leaf structure and gas exchange in California redwoods. Plant Cell Environ 32:743–757

Ambrose AA, Sillett SC, Koch GW, Van Pelt R, Antoine ME, Dawson TE (2010) Effects of height on treetop transpiration and stomatal conductance in coast redwood (*Sequoia sempervirens*). Tree Physiol 30:1260–1272

Ashton DH (2000) The environment and plant ecology of the hume range, Central Victoria. Proc R Soc Vic 112:185–278

Ashton DH, Chinner JH (1999) Problems of regeneration of the mature *Eucalyptus regnans* (the big ash) forest, in the absence of fire at Wallaby Creek, Victoria, Australia. Aust For 62:265–280

Australian Bureau of Meteorology (2007) Trend maps: trend in annual total rainfall for Victoria. Commonwealth of Australia Bureau of Meteorology, Melbourne. http://www.bom.gov.au/cgi-bin/silo/reg/cli_chg/trendmaps.cgi

Becker P, Meinzer FC, Wullschleger SD (2000) Hydraulic limitation of tree height: a critique. Funct Ecol 14:4–11

Buckley TN, Roberts DW (2006a) DESPOT, a process-based tree growth model that allocates carbon to maximize carbon gain. Tree Physiol 26:639–669

Buckley TN, Roberts DW (2006b) How should leaf area, sapwood area, and stomatal conductance vary with tree height to maximize growth? Tree Physiol 26:145–157

Callaway RM, Sala A, Keane RE (2000) Succession may maintain high leaf area: sapwood area ratios and productivity in old subalpine forests. Ecosystems 3:254–268

Connor DJ, Legge NJ, Turner NC (1977) Water relations of mountain ash (*Eucalyptus regnans*) forests. Aust J Plant Physiol 4:753–762

Das A, Stephenson NL, Flint A, Das T, van Mantgem PJ (2013) Climatic correlates of tree mortality in water- and energy-limited forests. PLoS One 8(7):e69917. doi:10.1371/journal.pone.0069917

Delzon S, Sartore M, Burlett R, Dewar R, Loustau D (2004) Hydraulic responses to height growth in maritime pine tree. Plant Cell Environ 27:1077–1087

England JR, Attiwill PM (2007) Changes in sapwood permeability and anatomy with tree age and height in the broad-leaved evergreen species *Eucalyptus regnans*. Tree Physiol 27:1113–1124

Ethier GJ, Livingston NJ (2004) On the need to incorporate sensitivity to CO_2 transfer conductance into the Farquhar–von Caemmerer–Berry photosynthesis model. Plant Cell Environ 27:137–153

Gerrish G (1990) Relating carbon allocation patterns to tree senescence in *Metrosideros* forests. Ecology 71:1176–1184

Ishii HR, Azuma W, Kuroda K, Sillett SC (2014) Pushing the limits to tree height: could foliar water storage compensate for hydraulic constraints in *Sequoia sempervirens*? Funct Ecol 28:1087–1093. doi:10.1111/1365-2435.12284

Keith H, Mackey BG, Lindenmayer DB (2009) Re-evaluation of forest biomass carbon stocks and lessons from the world's most carbon-dense forests. Proc Natl Acad Sci USA 106:11635–11640

Kilinc M, Beringer J, Hutley LB, Haverd V, Tapper N (2012) An analysis of the surface energy budget above the world's tallest angiosperm forest. Agric For Meteorol 166–167:23–31

Koch GW, Sillett SC, Jennings GM, Davis SD (2004) The limits to tree height. Nature 428:851–854

Köstner B, Falge E, Tenhunen JD (2002) Age-related effects on leaf area/sapwood area relationships, canopy transpiration and carbon gain of Norway spruce stands (*Picea abies*) in the Fichtelgebirge, Germany. Tree Physiol 22:567–574

Langford KJ (1976) Change in yield of water following a bushfire in a forest of *Eucalyptus regnans*. J Hydrol 29:87–114

Latham P, Tappeiner J (2002) Response of old-growth conifers to reduction in stand density in western Oregon forests. Tree Physiol 22:137–146

Legge NJ (1985) Relating water potential gradients in mountain ash (*Eucalyptus regnans*) to transpiration rate. Aust J Plant Physiol 12:89–96

Lindenmayer DB, Cunningham RB, Donnelly CF, Franklin JF (2000) Structural features of old-growth Australian montane ash forests. For Ecol Manag 134:189–204

Lindenmayer DB, Laurance WF, Franklin JF (2012) Global decline in large old trees. Science 338:1305–1306

Long JN, Smith FW (1988) Leaf area–sapwood area relations of lodgepole pine as influenced by stand density and site index. Can J For Res 18:247–250

Magnani F, Mencuccini M, Grace J (2000) Age-related decline in stand productivity: the role of structural acclimation under hydraulic constraints. Plant Cell Environ 23:251–263

McDowell NG, Barnard HR, Bond BJ, Hinckley TM, Hubbard RM, Ishii H, Köstner B, Meinzer FC, Marshall JD, Magnani F, Phillips N, Ryan MG, Whitehead D (2002a) The relationship between tree height and leaf area:sapwood area ratio. Oecologia 132:12–20

McDowell NG, Phillips N, Lunch C, Bond BJ, Ryan MG (2002b) An investigation of hydraulic limitation and compensation in large, old Douglas-fir trees. Tree Physiol 22:763–774

McDowell NG, Brooks JR, Fitzgerald SA, Bond BJ (2003) Carbon isotope discrimination and growth response of old *Pinus ponderosa* trees to stand density reductions. Plant Cell Environ 26:631–644

Medhurst JL, Beadle CL (2002) Sapwood hydraulic conductivity and leaf area–sapwood area relationships following thinning of a *Eucalyptus nitens* plantation. Plant Cell Environ 25:1011–1019

Mokany K, McMurtrie RE, Atwell BJ, Keith H (2003) Interaction between sapwood and foliage area in alpine ash (*Eucalyptus delegatensis*) trees of different heights. Tree Physiol 23:949–958

Petit G, Pfautsch S, Anfodillo T, Adams MA (2010) The challenge of tree height in *Eucalyptus regnans*: when xylem tapering overcomes hydraulic resistance. New Phytol 187:1146–1153

Phillips NG, Bond BJ, McDowell NG, Ryan MG (2002) Canopy and hydraulic conductance in young, mature and old Douglas-fir trees. Tree Physiol 22:205–211

Phillips NG, Buckley TN, Tissue DT (2008) Capacity of old trees to respond to environmental change. J Integr Plant Biol 50(11):1355–1364

Ryan MG, Yoder BJ (1997) Hydraulic limits to tree height and growth. Bioscience 47:235–242

Ryan MG, Phillips N, Bond BJ (2006) The hydraulic limitation hypothesis revisited. Plant Cell Environ 29:367–381

Sillett SC, Van Pelt R, Koch GW, Ambrose AR, Carroll AL, Antoine ME, Mifsud BM (2010) Increasing wood production through old age in tall trees. For Ecol Manag 259:976–994

Sillett SC, Van Pelt R, Carroll AL, Kramer RD, Ambrose AR, Trask D (2015) How do tree structure and old age affect growth potential of California redwoods? Ecol Monogr (in press)

Thomas SC (2011) Age-related changes in tree growth and functional biology: the role of reproduction. In: Meinzer FC, Lachenbruch B, Dawson TE (eds) Size- and age-related changes in tree structure and function. Springer, New York, pp 33–64

Tng DYP, Williamson GJ, Jordan GJ, Bowman DMJS (2012) Giant eucalypts—globally unique fire-adapted rain-forest trees? New Phytol 196:1001–1014

Van Mantgem PJ, Stephenson NL, Byrne JC, Daniels LD, Franklin JF, Fule PZ, Harmon ME, Larson AJ, Smith JM, Taylor AH, Veblen TT (2009) Widespread increase of tree mortality rates in the western United States. Science 323:521–524

Van Pelt R, Sillett SC, Nadkarni NM (2004) Quantifying and visualizing canopy structure in tall forests: methods and a case study. In: Lowman MD, Rinker HB (eds) Forest canopies, 2nd edn. Academic, New York, pp 49–72

Van Pelt R, Sillett SC (2008) Crown development throughout the lifespan of coastal *Pseudotsuga menziesii*, including a conceptual model for tall conifers. Ecol Monogr 78:283–311

Vertessy RA, Benyon RG, O'Sullivan SK, Gribben PR (1995) Relationship between stem diameter, sapwood area, leaf area, and transpiration in a young mountain ash forest. Tree Physiol 15:559–567

Wagenmakers E-J, Farrell S (2004) AIC model selection using Akaike weights. Psychon Bull Rev 11:192–196

West GB, Brown JH, Enquist BJ (1999) A general model for the structure and allometry in woody plants. Nature 400:664–667

Whitehead D, Beadle CL (2004) Physiological regulation of productivity and water use in *Eucalyptus*: a review. For Ecol Manag 193:113–140

Whitehead D, Edwards WRN, Jarvis PG (1984) Conducting sapwood area, foliage area, and permeability in mature trees of *Picea sitchensis* and *Pinus contorta*. Can J For Res 14:940–947